Click here to view PowerPoint presentation; Press Esc to exit

Store Separation Simulation of the Penguin Missile from Helicopters

Daniel J. Lesieutre, Marnix F.E. Dillenius
Nielsen Engineering & Research, Inc.
Mountain View, CA
USA

lesieutre@nearinc.com / mfed@nearinc.com

Jens A. Gjestvang
Kongsberg Defence & Aerospace AS
Kongsberg
NORWAY

jens.gjestvang@kongsberg.com

ABSTRACT

Under contract to Kongsberg Defence & Aerospace (KDA), Nielsen Engineering & Research (NEAR) combined and extended store separation simulation code NEAR STRLNCH and aerodynamic prediction code NEAR MISDL to simulate and analyze launch and separation of the KDA Penguin missile from a helicopter. One of the objectives was to enable the running of many cases in relatively short time on readily available computer platforms. The resulting MISDL/KDA code was validated by comparing to available free stream wind tunnel data as a function of component buildup and for a variety of wing deployment geometries. The combined launch simulation method STRLNCH/KDA with MISDL/KDA was validated by comparing predictions to flight test data.

LIST OF SYMBOLS

C_A	axial force/$q_\infty S_R$	q_∞	freestream dynamic pressure
C_D	drag force/$q_\infty S_R$	S_R	reference area
C_l	rolling moment/$q_\infty S_R l_R$; positive right wing down viewed from rear	x,y,z	fuselage coordinate system; origin at the nose
C_m	pitching moment/$q_\infty S_R l_R$; positive nose up	α	angle of attack, deg
C_n	yawing moment/$q_\infty S_R l_R$; positive nose right	α_c	included angle of attack, deg
C_N	normal force/$q_\infty S_R$	β	angle of sideslip, deg
C_Y	side force/$q_\infty S_R$	δ	canard deflection angle, deg
l_R	reference length	φ	roll angle, deg
M_∞	Mach number	Ψ,Θ,Φ	Euler angles; yaw, pitch, roll
p,q,r	rotational rates, roll, pitch, yaw		

1.0 INTRODUCTION

The Penguin missile was originally developed by KDA as a ship-to-ship missile. The Penguin 2 Mod 7 was developed for launch from helicopters such as the SH-60B; see Figure 1.

Lesieutre, D.J.; Dillenius, M.F.E.; Gjestvang, J.A. (2006) Store Separation Simulation of the Penguin Missile from Helicopters. In *Innovative Missile Systems* (pp. 9-1 – 9-18). Meeting Proceedings RTO-MP-AVT-135, Paper 9. Neuilly-sur-Seine, France: RTO. Available from: http://www.rto.nato.int/abstracts.asp.

Figure 1.- SH-60B helicopter releasing Penguin missile.

The original NEAR STRLNCH capability [1] models the parent aircraft, computes the flow field in which the store is immersed, and integrates the launched store trajectory as a function of time. Code extensions required to model Penguin launch included user-specified rotor wake, modeling characteristics unique to the canard-wing Penguin missile such as the effects of unfolding wings, hook release and delay, sway brace, lanyard and lanyard release, umbilical, wing roll tabs, time dependent thrust and mass properties, and the incorporation of a realistic autopilot. The modeling of the unique Penguin aerodynamics, including effects of fully and partially folded wings, was handled by the extended MISDL aerodynamic prediction code [2–5]. MISDL is based on panel and other singularity methods. The resulting code was designated STRLNCH/KDA.

2.0 TECHNICAL APPROACH

The following sections describe the theoretical methods incorporated in the MISDL and STRLNCH methodology.

2.1 Program MISDL

The intermediate-level MISDL code is based on panel methods and other singularity methods enhanced with models for nonlinear vortical effects [2–5]. The circular cross section body is modeled by sources/sinks and doublets for volume and angle of attack effects, respectively. If the body cross section is noncircular, a conformal mapping procedure is used to transform the noncircular cross section to a circular one. For the fin section, panel methods are employed to compute the lifting surface loadings. Nonlinear effects of body and fin wake vortices are modeled, and fin loads include simplified stall models. For subsonic flow conditions, the fin sections are modeled by a horseshoe-vortex panel method.

The MISDL solution proceeds in a stepwise manner from the body nose to the first fin section, through the first or forward fin section, the length of body from the first fin section trailing edge to the tail (or wing) section, the wing section, and finally the body section aft of the wing section to the base. A schematic of the stepwise procedure and panelling layouts is shown in Figure 2.

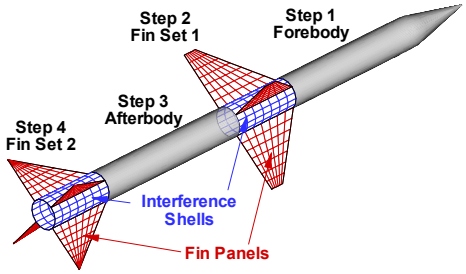

Figure 2.- MISDL modeling and solution procedure.

In the application to a body with fins, the body solution is performed first by module VTXCHN [6]. The VTXCHN module described below models circular and noncircular cross section bodies including those with chines. The fin section solution follows with the body-induced effects (perturbation velocities) included in the flow tangency boundary condition applied to the panels on the fins. This procedure is repeated in the case of a canard-tail fin configuration. Effects of vortical wakes from the nose and forward fin section are included in the length of body between the canard and tail section. The solution proceeds in a stepwise manner from the body nose, through the respective fin sections, to the base of the configuration as mentioned earlier. The MISDL methodology includes the capability to account for the effects of a nonuniform flow field in which the configuration may be immersed. Descriptions of the body and fin-section models follow.

2.1.1 VTXCHN Body Model

The VTXCHN body modeling methodology [6] predicts the aerodynamics of axisymmetric and noncircular body shapes using potential theory and conformal mapping techniques. The calculation proceeds as follows: 1) VTXCHN is used to compute the forebody loads including vortex shedding and tracking, 2) loads within the fin set are calculated including the effects of forebody vorticity, 3) the vorticity shed from the forebody and the forward fin set is included as an initial condition in VTXCHN which tracks and models additional vortices shed from the afterbody (length of body between forward and tail fin sets), and 4) if a second fin set is present, steps 2 and 3 are repeated.

The aerodynamic analysis of a body by VTXCHN comprises conformal mapping [7], elements of linear and slender body theory, and nonlinear vortical modeling. The analysis proceeds from the nose to the base. The body is sliced into many cross sections which are transformed to corresponding circles in the mapped plane. As a result, an axisymmetric body is created in the mapped space. If the actual body is axisymmetric, this step is omitted. In either case, the axisymmetric body is modeled by 3-D sources/sinks for linear volume effects and by 2-D doublets for linear upwash/sidewash effects.

At the first cross section in the mapped plane, velocity components are computed at points on the transformed (axisymmetric) body and transformed back to the physical plane. If the actual cross section has sharp corners or chine edges, vortices (with strengths determined later) are positioned slightly off the body close to the corner or chine points in the crossflow plane. The circumferential pressure distribution is determined in the physical plane using the compressible Bernoulli expression. For smooth cross sectional contours, the code makes use of the Stratford separation criteria [8] applied to the pressure distribution to determine the separation or vortex shedding points. The locations of the shed vortices are transformed to the mapped plane. The strengths of the shed vortices are related to the imposition of a stagnation condition at the separation points in the mapped plane. The vortices are then tracked aft to the next cross section in the mapped plane.

The procedure for the first cross section is repeated. The pressure distribution calculated at the second cross section in the physical plane includes nonlinear effects of the vortices shed from the first cross section. After the pressure distributions have been determined for all cross sections, the aerodynamic forces and moments are obtained by integrating the pressures. At the end of the body, the vortical wake is represented by a cloud of point vortices with known strengths and positions.

2.1.2 Fin Section Model

Program SUBDL [2] combined with the VTXCHN module can analyze an arbitrary cross section body with a maximum of two fin sections in subsonic flow. SUBDL and VTXCHN are included as modules in the MISDL/KDA software. The fins may be located off the major planes, and they can be at arbitrary angles to the body surface. The tip chord (if any) need not be parallel to the root chord. The code allows the fins to be in planar, triform, cruciform, or nonconventional (low observable) layouts. The axisymmetric body in the mapped plane (performed by body module VTXCHN) is modeled with subsonic 3-D sources and sinks to account for volume effects, and by 2-D doublets for angle-of-attack effects. The lifting surfaces and the portions of the body spanned by the lifting surfaces, the interference shell, are modeled with planar subsonic lifting panels called horseshoe vortex panels. The strengths of the body and lifting surface singularities are obtained from different sets of linear simultaneous equations based on satisfying the flow tangency condition at a set of discrete aerodynamic control points. The body solution is performed first, and the panel solutions for the canard and tail fins proceed in a stepwise manner. In this process, body-on-fin interference is included, and fin-on-body lift carryover is modeled by the interference shells. The fin section modeling procedure is detailed below.

2.1.2.1 Vortex Lattice Model

The vortex lattice method in MISDL/KDA models the fins and body of a fin section by covering the configuration with a set of discrete panels. As part of the work performed under contract to KDA, the major modifications and extensions made to the MISDL code included the capability to handle folded and partially deployed wings. This involved extending the geometry of the lifting surfaces to allow for changes in dihedral as a function of span. In addition, the root chord of the canard fins was made to conform with the nose meridional shape. In order to accomplish this, the layout of the panels on the fins was modified to handle curvature. These features are shown in Figure 3.

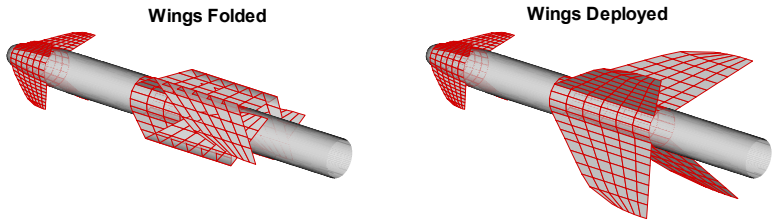

Figure 3.- MISDL fin modeling for the Penguin missile.

Typically, a vortex lattice panel is composed of a bound vortex segment placed on the ¼ chord of each panel and trailing vortices which extend from the bound segment endpoints back to infinity in the axial direction. To model a fin on a nose (or boattail), where the panel side edges are not in the axial direction, the trailing vortex from each bound segment endpoint must be modeled as a set of bound segments along the panel side edges; at the trailing edge the trailing segments are then assumed to go to infinity in the axial direction. The vortex lattice modeling of fins on a nose is depicted in Figure 4 .

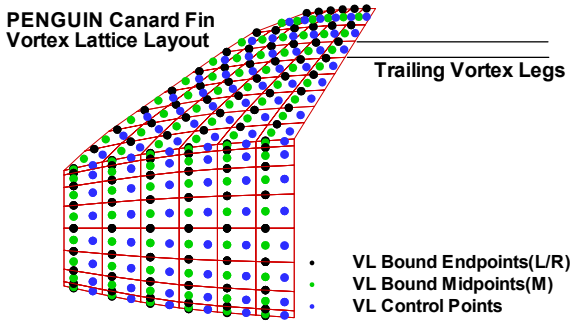

Figure 4.- Fin section vortex-lattice modeling

The vortex lattice modeling for the Penguin wings has been modified to allow for a fold line and fold angle. For all panels, control points for the vortex lattice system are located midway between the trailing vortex legs at the 75-percent panel chord location. The fins in a fin section are modeled with a set of planar horseshoe vortices. The bound vortex and its trailing vortices are planar. For cases where the wings are folded, a panel edge is forced at the fold line. Therefore, the individual panels are planar inboard and outboard of the fold line. The horseshoe vortices in the interference shell around the body are used only to model the carryover forces between the body and fins (body volume and angle of attack effects are included in the 3-D sources and doublets and conformal mapping procedure). The strengths of the vortex lattice panels are obtained from a set of linear simultaneous equations based on satisfying the flow tangency condition at the control points. This is formulated by enforcing the dot-product of the total velocity and the normal vector at each control point to be zero.

2.1.2.2 .Nonlinear Effects on the Fins

Fins can develop leading- and side-edge separation vorticity as the angle of attack is increased. If the side edge of a given fin is long (similar in length to the root chord, for example), vorticity can be generated along the side edge at angles of attack as low as 5 deg. The leading-edge and side-edge vortices may combine and form a pattern of strong vorticity located above the trailing edge as shown in Figure 5. This figure depicts how MISDL models the path of the combined leading- and side-edge vortex by locating it above the fin plane at an angle equal to one-half of the local angle of attack (as seen by the fin). In the case of a missile, the forward fins may generate leading- and/or side-edge vortices which stream aft along the afterbody and tail section and influence the pressures on those components.

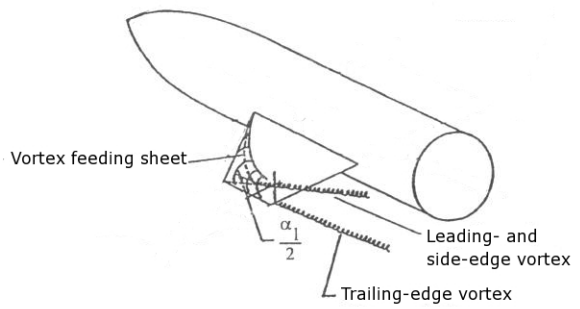

Figure 5.- Fin vortex modeling.

The vortical phenomena along the fin leading- and side-edges are accompanied by augmentation to fin normal force which is nonlinear with angle of attack seen by the fin. This nonlinearity is modeled by calculating the distribution of suction along the leading and side edges. In accordance with an extension [4] of the Polhamus suction analogy [9], the suction is converted to normal force in proportion to vortex lift factors. The result is a distribution of nonlinear, additional fin normal force along the leading and the side edge.

A fin stall model is included for more realistic prediction of fin forces above an approximately 10 deg angle of attack. This stall model is based on methods used in the *U.S. Air Force Stability and Control Datcom Handbook* [10]. The fin stall model compares predicted fin section lift coefficients to an empirical/data base maximum section lift coefficient model. This model is a function of the thickness to chord ratio (t/c), the location (x/c) of maximum thickness, the airfoil shape, and the Reynolds number based on local chord. If the predicted lift coefficient for a given section exceeds the stall lift coefficient, the horseshoe vortex strengths determined from the vortex lattice solution are adjusted (reduced) and used in the calculation of the fin forces.

2.1.3 Applicable Ranges

In the MISDL/KDA program, the valid range of Mach numbers is subsonic up to the onset of local supersonic flow (transonic effects). Fin-body angles of attack are generally limited to 30 deg. Angle of roll is arbitrary. Control fins may be deflected up to 20 deg with the upper limit depending on angle of attack; the sum of deflection angle and angle of attack should not exceed 40 deg. Effects of rotational rates and nonuniform flow are included in the methodology. If MISDL/KDA is used to calculate the aerodynamic loads acting on the launched store, the methodology includes perturbation velocities induced by the parent aircraft.

2.2 Program STRLNCH

The STRLNCH store separation simulation software is based on 1) modeling the flow field of a parent aircraft including fixed stores, 2) modeling the aerodynamics of the released store, and 3) integration of the six-degree-of-freedom equations of motion for the released store.

Figure 1 depicts a schematic of the helicopter with the Penguin missile in the carriage position. The modeling of the helicopter flow field and specific Penguin characteristics are described next. Comparisons of predicted trajectories with flight test data are presented in a later section. Modifications to the STRLNCH software required in this effort are described below.

The STRLNCH subsonic store separation code [1] was used as the starting point in the development of the STRLNCH/KDA code for predicting trajectory characteristics of the Penguin missile released from a helicopter. The aircraft flow models are composed of module VTXCHN (see earlier section) for modeling the aircraft fuselage including vortex shedding and a vortex lattice for modeling both the wing/pylon and the interference shell for wing-on-fuselage aerodynamic interference.

The STRLNCH code is capable of modeling flow effects due to combined angle of pitch and sideslip as well as rotational rates of the parent aircraft. The store or missile aerodynamic loading calculation method was upgraded by using an enhanced version of the NEAR MISDL panel method-based missile aerodynamic prediction code described above. This aerodynamic module provides the store aerodynamics for use in the STRLNCH 6-DOF trajectory calculations.

The flow models in the STRLNCH program are valid for subsonic Mach numbers (greater than zero) up to the critical speed or onset of transonic flow. The flow models represent effects of lift and thickness. Details of the

horseshoe panel and other singularity-based flow models are described in References [11] through [13]. Program STRLNCH includes first-order corrections to the wing horseshoe vortex panel method to account for high angle-of-attack effects. This includes a semi-empirical stall model to modify the wing horseshoe vortex panel strengths at high angles of attack.

A given fuselage and wing/pylon(s) combination is treated by solving first the fuselage alone and fixed stores (if any). A solution of the wing/pylon(s) and interference shell is then obtained with the fuselage and fixed store effects included in the flow tangency condition applied at the control points of the horseshoe vortex panels on the wing/pylon(s). In this way, the fuselage and fixed stores interfere on the wing/pylon(s), and the wing/pylon(s) interfere on the fuselage via the interference shell.

With the strengths of the singularities used to model the aircraft known, the flow field in the vicinity of any attached store is calculated. The parent aircraft perturbation velocities are then passed to the MISDL aerodynamic prediction method, and the store loads are calculated, including parent aircraft effects. The store is then moved to its next position under the influence of the calculated aerodynamic loads over a short integration time interval. The aerodynamic loads are recalculated and the store is moved to its next position. This process is repeated until the trajectory calculation is stopped.

2.2.1 Major Enhancements

Enhancements made for KDA to the STRLNCH and MISDL codes to model the Penguin release from helicopters include 1) helicopter rotor wake model, 2) hook release and hook delay model, 3) swaybrace forces and moments, 4) umbilical forces and moments, 5) Penguin autopilot model, 6) Penguin canard fin actuator model, 7) lanyard length model, 8) lanyard release model - release pin "pull-force," 9) Penguin wing deployment dynamics model, and 10) Penguin roll-tab rolling moment model. Further details of these enhancements follow.

2.2.1.1 Helicopter Rotor Wake Model

The inclusion of a specified helicopter rotor wake model is an enhancement to the parent aircraft flow field model. Three methods for the user to specify the helicopter rotor wake have been implemented.

1. The simplest wake specifies a swept cylinder in which the wake downwash is constant. The center of the rotor wake, the wake radius, the sweep of the wake centerline, and a uniform downwash velocity are specified.
2. The second rotor wake input allows for a radial variation in downwash. The rotor wake geometry is a swept cylinder like the first option. However, the user can read in a downwash velocity that is a function of the radius from the hub to the tip of the rotor.
3. The third wake option is the most general and allows for an arbitrary wake to be specified which is a function of vertical, radial, and circumferential coordinates.

In any of the three methods, the mutual interference between the oncoming flow and the rotor wake is not accounted for.

2.2.1.2 Hook Release and Hook Delay Model

A hook release delay model is implemented. Two hooks can be modeled. One of the two hooks can be specified to release after a delay. The hook delay is formulated by enforcing the acceleration of the Penguin

to be zero at the hook attachment point. The Penguin is free to drop/rotate subject to the constraint that the hook point is stationary. During the hook delay portion of the trajectory, there are three (3) additional state constraint equations which are integrated with the 6-DOF trajectory equations to ensure zero acceleration of the hook point. In addition, a hook breaking force can be specified. If the hook constraining force exceeds the hook breaking force, the hook is released.

2.2.1.3 Swaybrace Forces and Moments

Based on sway-brace forces supplied by KDA, NEAR developed a two-degree-of-freedom model (vertical z position and angle from vertical θ) for the forces and moments. The swaybrace forces are assumed to act at a constant position and orientation on the Penguin, and are assumed to be a linear function of the two state variables z and θ. The forces are assumed to act quickly (approx. 0.005 sec.), and aerodynamic forces are neglected. The equations of motion are integrated until the store falls clear of the last swaybrace. The change in states due to the swaybrace forces are used as initial conditions for the trajectory calculations.

2.2.1.4 Umbilical Forces and Moments

KDA specified the Penguin umbilical force versus vertical position. This umbilical has been modeled as an ejector in STRLNCH. The z-position is measured perpendicular to the missile centerline. When the missile is in carriage, z = 0. This functionality is included to investigate effects of failure of the Umbilical Retraction Unit (URU) in the bomb rack or of possible icing in the interface between the connector and the missile.

2.2.1.5 Penguin Autopilot Model

The Penguin autopilot subroutine used in the STRLNCH/KDA software is derived from the actual flight software. Changes have been made to exclude parts that are not related to the separation part of the flight and some simplifications have been introduced. The simplified routine has been compared to the full autopilot by using KDA's own simulation tools. The performance in the separation phase is for all practical purposes identical to the performance of the actual missile autopilot software. The autopilot consists of a PID controller with gain scheduling based on launch velocity and certain Euler angle considerations. The autopilot only controls azimuth and pitch since the missile is constantly rolling in flight due to fixed roll tabs on the wings. The simulation software allows for changes in the autopilot by compiling and linking the subroutine to the precompiled parts of the STRLNCH/KDA software.

The autopilot which commands canard fin control deflections is active prior to the release from the helicopter and is critical to modeling launch trajectory characteristics. For the launch phase, the autopilot logic commands deflections such that the initial heading of the Penguin is maintained.

2.2.1.6 Penguin Actuator Model

KDA supplied diagrams for a second-order actuator model including deflection angle, rate, and acceleration limiters. The actuator model was implemented in mathematical modeling software, and verified against KDA-supplied properties and step responses. A subroutine was written, verified and included in STRLNCH/KDA. The actuator model results in four (4) additional equations to be integrated with the standard 6-DOF equations for the launched store. There are two equations for the azimuth and two for the pitch channels of the autopilot. The input to the actuator model is the commanded deflections computed by the autopilot. The output is the actual fin deflections which are passed to MISDL/KDA to compute the aerodynamic forces at given instants of time during the trajectory calculation.

2.2.1.7 Lanyard Length Model

In order to determine when wing unfolding for deployment begins, a lanyard model is implemented. The lanyard for each Penguin wing is characterized by its attachment points to the helicopter and to the missile, and by its maximum deployed length. As part of the simulation, STRLNCH/KDA tracks the deployed length of each of the four (4) wing lanyards. When the maximum deployed length is reached, a release pin "pull-force" model is applied and wing deployment begins. For the flight test results presented (results section), a fifth lanyard is modeled associated with the Flight Termination System (FTS) system.

2.2.1.8 Lanyard Release Model - Release Pin "pull-force"

During the pulling of the wing fold release pins, forces are applied to the Penguin through the lanyard. To model these forces, KDA supplied a specification of the force required to pull the pin. In STRLNCH/KDA it is assumed that: 1) the lanyard release event acts quickly, 2) the store orientation and mass are constant during the event, and 3) the lanyard forces and moments can be modeled as impulses.

The impulse model computes the change in translational and rotational velocities of the missile due to the pulling of each pin. These velocities are added as an increment to corresponding state variables for the store in the trajectory calculation.

2.2.1.9 Penguin Wing Deployment Dynamics Model

The unfolding mechanism of the Penguin wings consists of a spring and damper. The modeled dynamics of the Penguin wing deployment are based on a KDA Supplied Report [14]. The equations of motion for the wing deployment angles and rates were implemented in mathematical software for testing. These equations of motion include mass, inertia, deploying spring, and arresting damper terms. The results were verified against the KDA report, and a subroutine was written and verified.

The wing deployment routine was considered for direct inclusion in the simulation equations of motion (as additional states). However, parametric studies performed with the deployment model indicated that the deployment of the wings is dominated by the spring and damper characteristics and that the missile states (ϕ and p, roll angle and roll rate) are only affected during the deployment. Conversely, the missile states (ϕ and p) and aerodynamic effects only have a second- or higher-order effect on the wing deployment states (fold angle and unfolding rate). Additionally, the inclusion of the impulsive stopping of the wing deployment when the wing locks into place has the following effects: 1) the net imparted roll rate after deployment is 0.0, and 2) the net roll angle change after all 4 fins are deployed is nearly zero. It is not exactly zero because of the different fold angles.

Therefore, the modeling of the wing deployment dynamics through additional equations of motion in the simulation is not necessary or practical since the net effect on roll angle and roll rate is zero once all fins are deployed. For the simulation, the effects of each wing deploying on the missile roll angle, rate, and acceleration are stored in tabular format (versus time after deployment begins). These tables are read into the simulation. Table lookup is used for each wing individually and summed to get the overall effects on the missile states.

2.2.1.10 Penguin Roll Tab Rolling Moment Model

The Penguin wings have roll tabs which force the vehicle to roll. A direct method of modeling Penguin roll tabs is currently not implemented in MISDL/KDA. This would require a panel layout which had panels specifically laid out on the roll tabs which could be deflected. To include the effects of roll tabs in the simulation, a Mach number dependent variation of wing roll tab rolling moment is read into the code. The KDA Low-Speed Wind Tunnel Data [15] does not provide a good model of the roll tab rolling moments. There is no Mach number effect and there is a variance between different tunnel tests.

Instead of the above, NEAR used the KDA Flight Test Data to formulate an empirical variation of tab rolling moment versus Mach number. This variation is shown in Figure 6 and provided the best agreement with the flight characteristics.

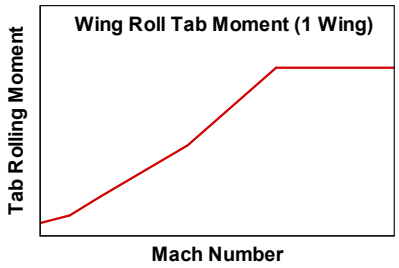

Figure 6.- Penguin wing tab rolling moment.

The empirical roll tab model is included as an input item for the MISDL/KDA aerodynamic module. For each fin, the individual characteristics of a roll tab can be specified, including 1) the spanwise roll tab position, and 2) the roll tab moment as a function of Mach number. This allows individual fins to have different roll tabs and allows an approximation for the effect of the wing fold angle on the roll tab effectiveness.

3.0 RESULTS

The first portion of this section describes comparisons between the MISDL/KDA predictions and wind tunnel data for freestream aerodynamic characteristics of the Penguin missile. This is followed by comparisons between STRLNCH/KDA (with MISDL/KDA) predictions and flight test data for the Penguin launched from the SH-60 helicopter.

3.1 Freestream Aerodynamics for Penguin Configuration

Free stream characteristics predicted by MISDL/KDA will be described next. Figure 1 shows the Penguin missile immediately after release from an SH-60 helicopter. Some details of the missile are visible in the insert. The MISDL/KDA predictions were tested against low speed wind tunnel data for the Penguin in free stream.

Results obtained with the MISDL/KDA code are compared to low speed wind tunnel data [15] for the Penguin missile in Figure 7 through Figure 12. For KDA company proprietary reasons, certain details in the axes can not be shown. Results are shown over a realistic range in angle of attack. In the wind tunnel tests, the Penguin missile was tested in the "X" orientation (rolled 45 deg). For this case, the forces and moments are expressed in the unrolled body coordinate system: C_N up, C_Y to right.

MISDL/KDA predictions were compared to available component buildup wind tunnel data. The configurations tested are depicted in Figure 7. The letter B denotes body alone, BC means canard fins on the body, E/BW means fully deployed wings on the body, E/BWC stands for canard fins and fully deployed wings on the body.

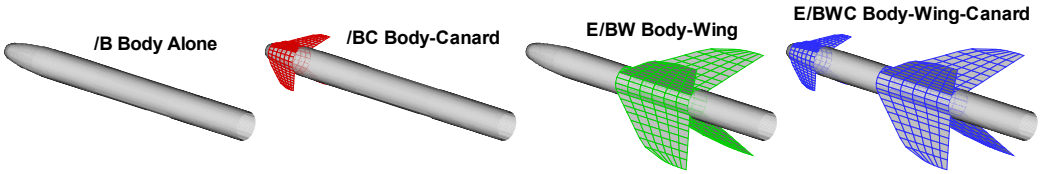

Figure 7.- Component Buildup Configurations.

The component buildup normal force and drag characteristics are shown in Figure 8, and the pitching moment and center-of-pressure location are shown in Figure 9. In general, the effects of adding components as predicted by MISDL/KDA agree well with the experimental data. For the body alone, it is interesting to note the travel of center-of-pressure from near the nose to a midbody position as angle of attack increases.

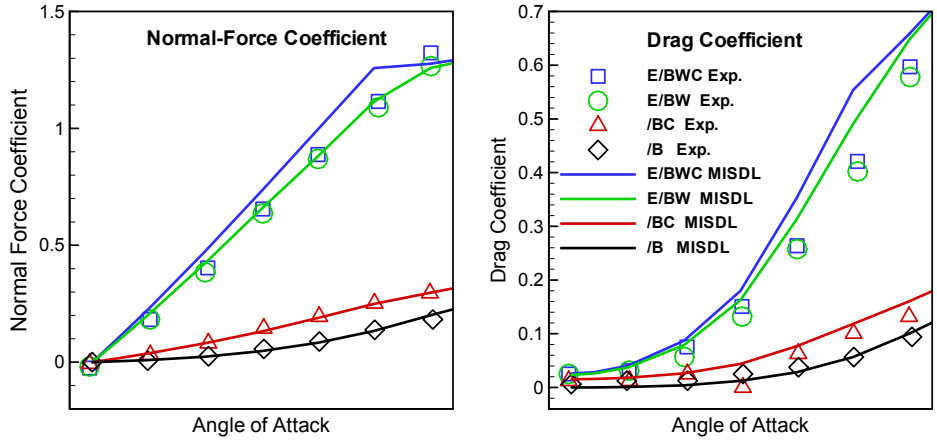

Figure 8.- Penguin component buildup normal force and drag characteristics.

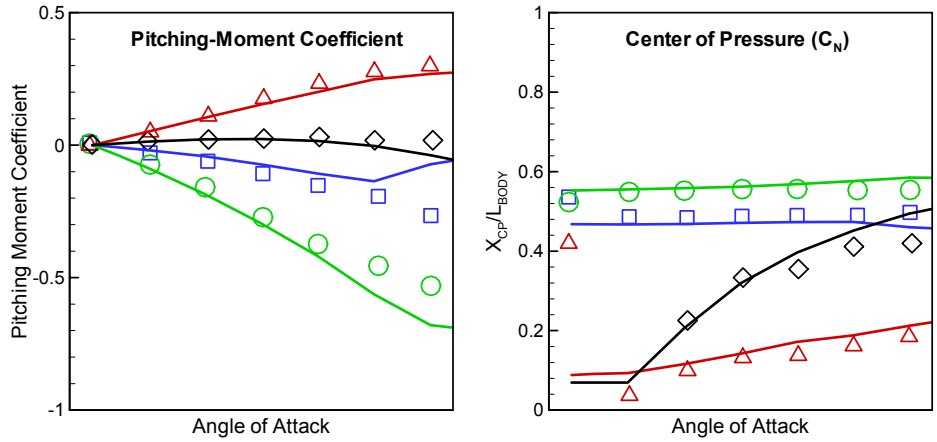

Figure 9.- Penguin component buildup pitching moment and center-of-pressure characteristics.

The unique effects of wing deployment are shown next. Figure 10 depicts the wing deployment configurations modeled for which experimental data were available from completely folded denoted A to fully deployed denoted E. It is worth noting that the deployment scenarios not only affect the longitudinal aerodynamic characteristics but the lateral characteristics as well. The latter are particularly difficult to predict.

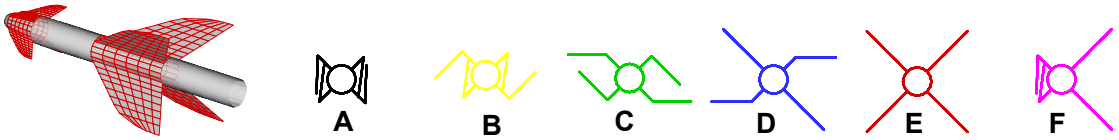

Figure 10.- Penguin wing deployment configurations.

Figure 11 compares measured and predicted normal force and pitching moment acting on the complete configuration BWC as a function of angle of attack over a realistic range for the wing deployment configurations depicted in Figure 10. Figure 12 compares side force, yawing moment, and rolling moment. In general, the MISDL/KDA code predicts the effects of the various deployed wing configurations reasonably to quite well.

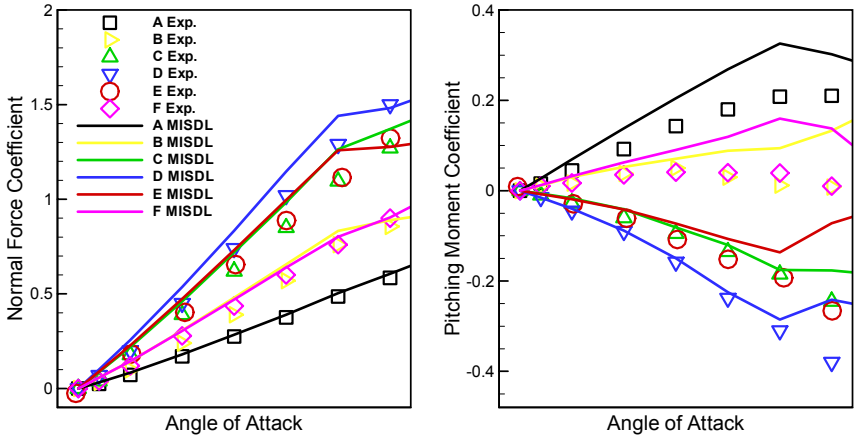

Figure 11.- Pitch-plane characteristics of the Penguin missile with wings in various deployment positions.

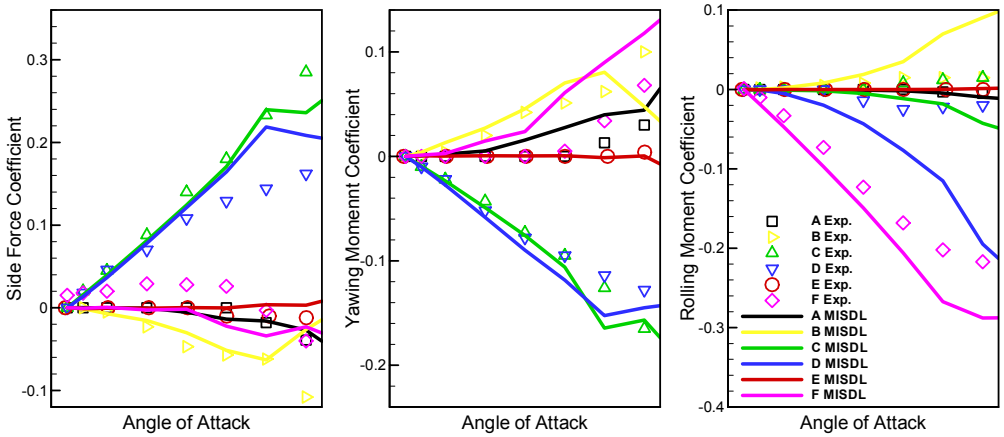

Figure 12.- Lateral-plane characteristics of the Penguin missile with wings in various deployment positions.

3.2 Penguin Launch Characteristics

The Penguin missile was launched from underneath a short pylon which was mounted to a short rectangular wing on the side of the SH-60 fuselage as shown schematically in Figure 13. The Penguin wings were folded at the start of the launch as shown in the figure. Flight test telemetry included downrange and vertical position, Euler angles and rotational rates. For the results presented in this paper, the graphs include vertical scale bars which indicate the magnitude of the plotted variable; specific values are not shown for KDA proprietary reasons.

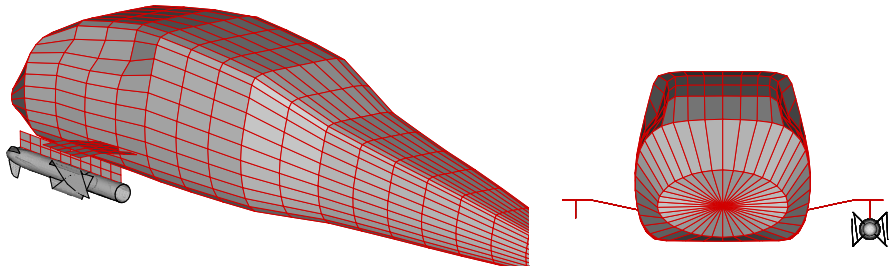

Figure 13.- Schematic of helicopter with Penguin missile in carriage position.

For Flight Test 01, the angle of attack and sideslip of the helicopter at launch were each approximately 2 deg. Launch flight Mach number was low. For this forward flight speed, it was assumed that the rotor wake lies aft of the Penguin and therefore was not modeled. The autopilot commanded a constant heading angle for the launch phase of the trajectory. The wing deployment and Flight Termination System (FTS) lanyards were modeled. In the STRLNCH/KDA simulation, the Penguin outboard wing lanyards pulled at t = 0.415 secs and the inboard pair pulled at t = 0.485 secs. In the simulations the rocket motor was ignited at t = 0.75 secs. Figure 14 presents the predicted and flight test downrange position and velocity, and Figure 15 depicts the vertical position and velocity. There is good agreement between the predicted and flight test results.

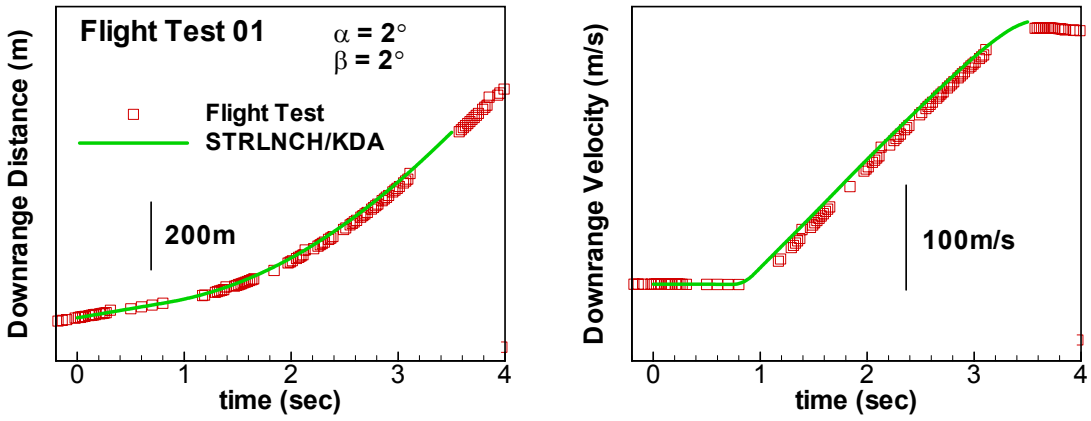

Figure 14.- Comparison of predicted and flight test downrange distance and velocity.

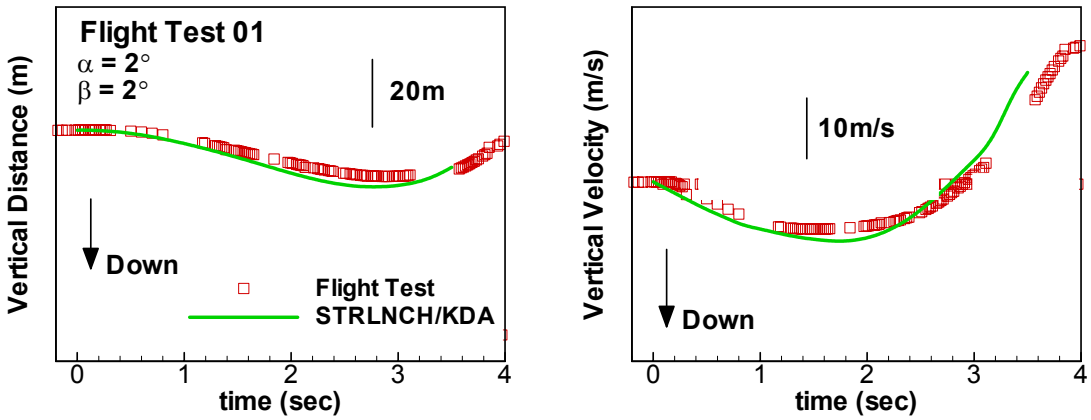

Figure 15.- Comparison of measured and flight test vertical position and velocity.

Figure 16 compares the Euler angles and the rotational rates. It is seen that the autopilot maintained the initial heading angle (ψ) and that the predicted roll characteristics are similar to the flight test data. The effects of the wing unfolding dynamics can be seen in the roll rate (p) graph. The magnitude and characteristics of the roll rate due to wing deployment matches the flight test but occurs slightly earlier.

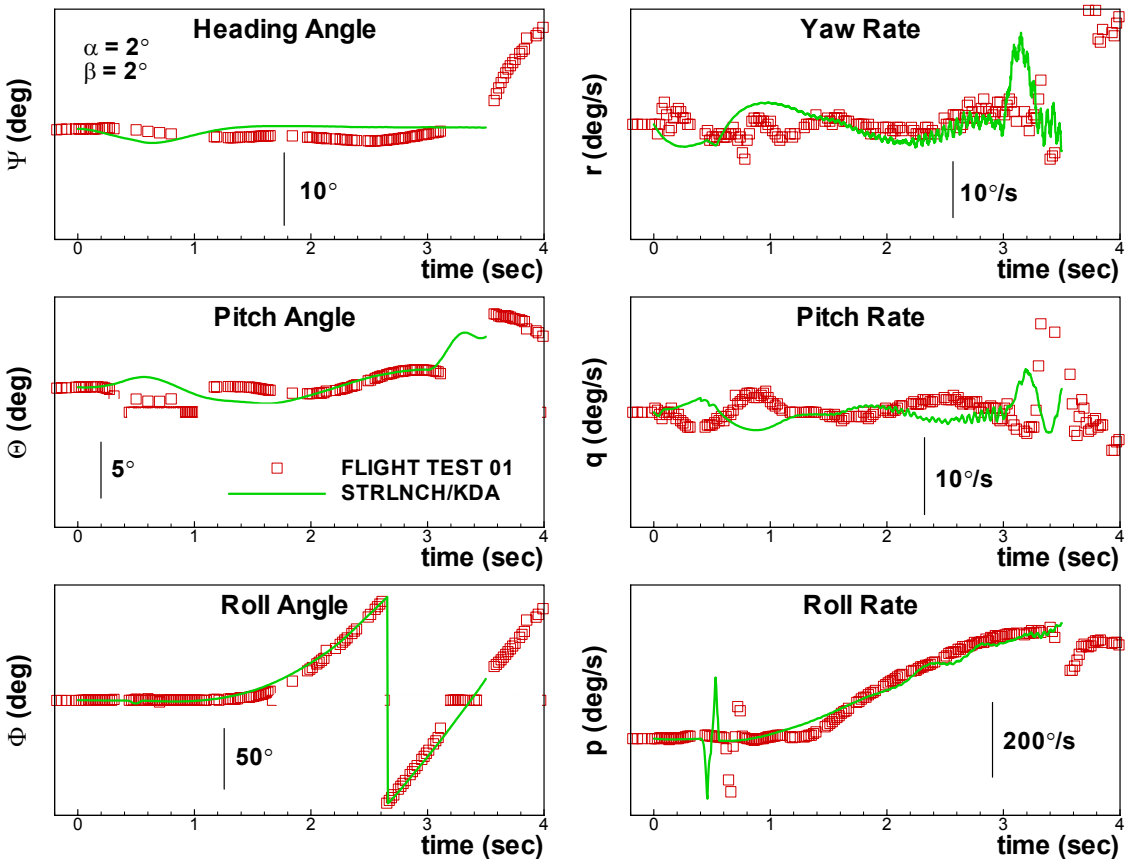

Figure 16.- Comparison of predicted and flight test Euler angles and rotational rates.

Figure 17 compares the Penguin angle of attack and angle of sideslip, and Figure 18 compares the commanded pitch and azimuth deflections and the actual canard control deflections. These characteristics are hard to predict and to measure. Angle of attack and sideslip are usually estimated quantities in a flight test. Because of the autopilot, the predicted and measured deflections are expected to be different for several reasons: 1) the flight test and predicted aerodynamics may not agree exactly for all times, 2) the parent aircraft flow model may not be exactly that of the actual helicopter, and 3) there may have been winds present not modeled in the simulation. Errors in any of these models will cause the autopilot to produce different deflections. However, the autopilot in both cases is working correctly as indicated in Figure 14 throughFigure 16. The vertical position is in good agreement, Figure 15, and the heading angle is maintained, Figure 16.

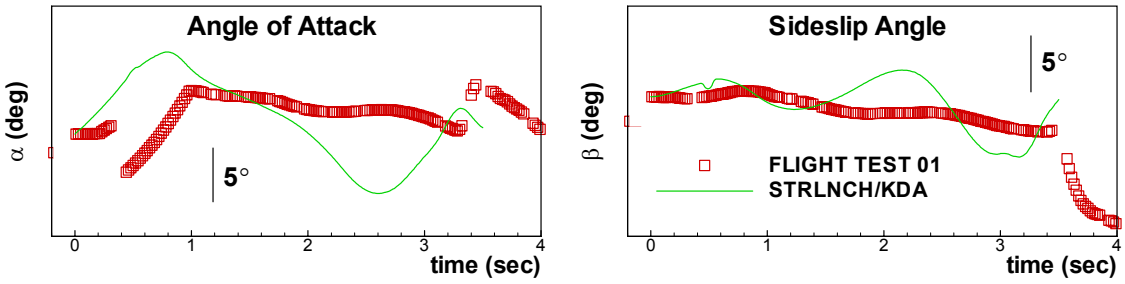

Figure 17.- Comparison of predicted and flight test estimated angle of attack and sideslip angle.

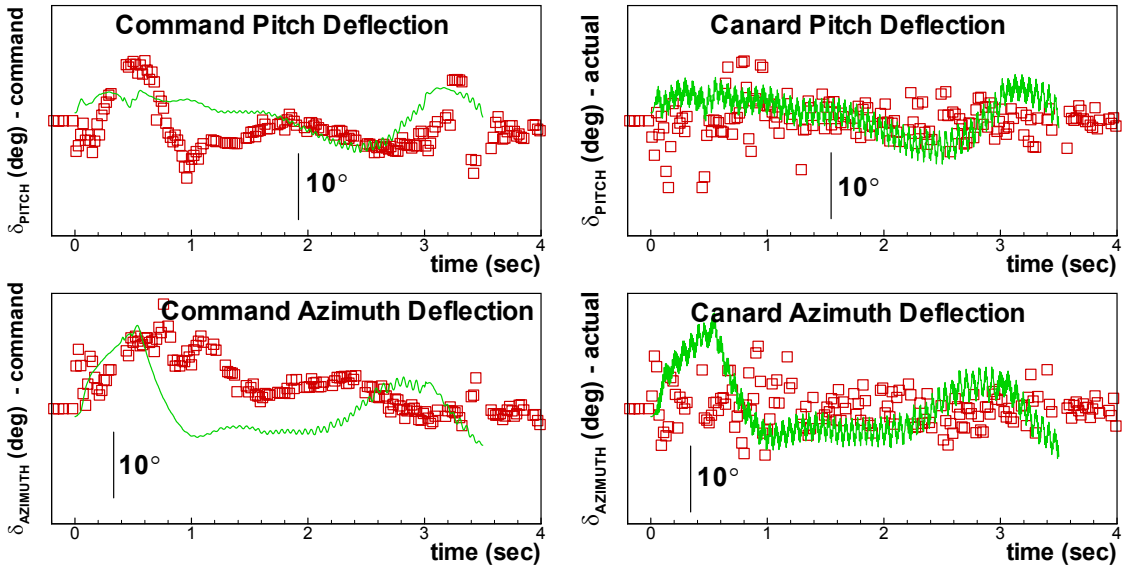

Figure 18.- Comparison of predicted and flight test commanded and actual fin deflections.

4.0 CONCLUSIONS

The store separation simulation code STRLNCH along with the intermediate-level missile aerodynamic prediction code MISDL have been adapted to model the launch and separation characteristics of the Kongsberg Defence & Aerospace (KDA) subsonic Penguin missile configuration from a helicopter. The extensions to the STRLNCH and MISDL codes required the modeling of several characteristics unique to the

Penguin. The paper describes how the resulting STRLNCH/KDA code handles the Penguin aerodynamics and the dynamics associated with the folded and unfolding wings, the wing unfolding inertial dynamics, the lanyard and lanyard release force effects, the wing roll tabs, the time-dependent thrust and mass properties, and the realistic autopilot. The prediction capability of the MISDL/KDA code is illustrated by comparisons with free stream wind tunnel data for the Penguin configuration. The STRLNCH/KDA simulation with MISDL/KDA Penguin modeling predict launch characteristics of the Penguin that agree well with flight test telemetry data. The simulation also allows for launch failure studies such as wing deployment failure and hook release delays.

5.0 ACKNOWLEDGMENT

The work reported herein was performed by Nielsen Engineering & Research under contract to Kongsberg Defence & Aerospace AS (KDA). The cognizant engineers at KDA were Mr. Jens A. Gjestvang and Mr. Helge Morsund.

6.0 REFERENCES

[1] Dillenius, M. F. E., Love, J. F., Hegedus, M. C., and Lesieutre, D. J., "Program STRLNCH, Simulation of Missile Launch From Maneuvering Aircraft at Subsonic or Supersonic Speeds," NEAR TR 509, Oct. 1996.

[2] Lesieutre, D. J., Dillenius, M. F. E., and Whittaker, C. H., "Program SUBSAL and Modified Subsonic Store Separation Program for Calculating NASTRAN Forces Acting on Missiles Attached to Subsonic Aircraft," NAWCWPNS TM 7319, May 1992.

[3] Dillenius, M. F. E., Perkins, S. C., Jr., and Lesieutre, D. J., "Modified NWCDM-NSTRN and Supersonic Store Separation Programs for Calculating NASTRAN Forces Acting on Missiles Attached to Supersonic Aircraft," Naval Air Warfare Center Report NWC TP6834, Sep. 1987.

[4] Lesieutre, D. J., Dillenius, M. F. E., and Lesieutre, T. O, "Multidisciplinary Design Optimization of Missile Configurations and Fin Planforms for Improved Performance," AIAA 98-4890, Sep. 1998.

[5] Dillenius, M. F. E., Lesieutre, D. J., Hegedus, M. C., Perkins, S. C., Jr., Love, J. F., and Lesieutre, T. O., "Engineering-, Intermediate- and High-Level Aerodynamic Prediction Methods and Applications," *Journal of Spacecraft and Rockets*, Vol. 36, No. 5, Sep.-Oct. 1999, pp. 609-620.

[6] Hegedus, M., Dillenius, M. F. E., and Love, J., "VTXCHN: Prediction Method For Subsonic Aerodynamics and Vortex Formation on Smooth and Chined Forebodies at High Alpha," AIAA 97-0041, Jan. 1997.

[7] Skulsky, R. S., "A Conformal Mapping Method to Predict Low-Speed Aerodynamic Characteristics of Arbitrary Slender Body Re-Entry Shapes," *Journal of Spacecraft and Rockets*, Vol. 3, No. 2, Feb. 1966, pp. 247-253.

[8] Stratford, B. S., "The Prediction of Separation of the Turbulent Boundary Layer," *Journal of Fluid Mechanics*, Vol. 5, 1959, pp. 1-16.

[9] Polhamus, E. C., "Prediction of Vortex-Lift Characteristics Based on a Leading-Edge Suction Analogy," *Journal of Aircraft*, Vol. 8, Apr. 1971, pp. 193-199.

[10] Hoak, D. E., et al, USAF Stability and Control DATCOM, McDonnell Douglas Corp., 1960, revised 1978.

[11] Goodwin, F. K., Dillenius, M. F. E., and Nielsen, J. N., "Extension of the Method of Predicting Six-Degree-of-Freedom Store Separation Trajectories at Speeds up to Critical Speed, Vol. I, Theoretical Methods and Comparison with Experiment," AFFDL-TR-72-83, 1972.

[12] Goodwin, F. K., Dillenius, M. F. E., and Nielsen, J. N., "Extension of the Method of Predicting Six-Degree-of-Freedom Store Separation Trajectories at Speeds up to Critical Speed to include a Fuselage with Non-Circular Cross Section," AFFDL-TR-74-130, Vol. I, 1974.

[13] Dillenius, M. F. E., Lesieutre, T. O., and Lesieutre, D. J., "Subsonic Parent Aircraft Flow Prediction Program SBPAFL," NEAR TR 485, Dec. 1994.

[14] "Penguin MK2 MOD7 Wing Deployment Analysis," Kongsberg Defence Products Division, Document No. FP207-UHK-22-0436, Mar. 1985.

[15] "Penguin MK2 MOD7 Low Speed Wind Tunnel Test Report," Kongsberg Defence & Aerospace AS., Document No. 01TR68072909, Jan. 1998.

SYMPOSIA DISCUSSION – PAPER NO: 9

Discusser's Name: CLOKE Malcolm

Question:
What type of helicopter rotor wake model did you use?

Author's Name: LESIEUTRE Daniel

Author's Response:
3 different kinds:

1) Simple downwash input, e.g. 10 ms-1 with swept wake
2) Radial model
3) Full user input 3 D grid method